

## OPTICAL POLARIZATION VARIABILITY OF THE M87 JET; AN IN-DEPTH LOOK AT THE HST-1 COMPONENT

MATTHEW BOURQUE<sup>1</sup>, ERIC PERLMAN, AND MIHAI CARA

Department of Physics and Space Sciences & the SARA Observatory, Florida Institute of Technology, Melbourne, FL 32901

### ABSTRACT

We present HST V band polarimetry observations of the M87 jet, ranging from 1995 to 2007 with greater sampling occurring during the 2005 flux outburst of innerknot HST-1. Our objective was the measure the fractional polarization of light emitted from the knot regions of the jet to check for variability. Our results showed that there was significant polarization variability in the core and the HST-1 knot. However, the magnetic field position angle of the core showed drastic changes whereas the PA of HST-1 was mostly constant. Large Polarization variability in the jet suggests a changing magnetic field that could indicate that jet dynamics or the addition of particles play a role in the giant 2005 flare of HST-1.

*Subject headings:* galaxies: individual (M87) - galaxies: active - galaxies: jets; nuclei

### 1. INTRODUCTION

M87, the giant elliptical galaxy located in the Virgo cluster, is host to a relativistic jet that is emitting material at speeds close to  $c$ . Because of M87's large size and proximity (distance of 16 Mpc), the jet has been observed at high resolution (angular scale of 1 arcsecond = 78 pc) and is an ideal candidate for modeling. Many studies have been done in radio, optical and X-ray wavelengths (Tsvetanov et al. 1998, Capetti et al. 2007, Harris et al. 2003, 2007, 2009, Perlman et al. 2003).

M87's core houses an Active Galactic Nucleus (AGN). In AGNs, material from the interstellar medium accretes onto the central supermassive black hole. Though the mechanisms behind it are still not completely understood, this material can get ejected in the form of a jet with the material moving at speeds up to  $0.99c$ . These speeds, coupled with the fact that observations are made looking down the jet due to its angle in our reference frame, lead to relativistic effects such as Doppler boosting. Such relativistic effects can affect the time scales of variability as well as overall luminosity. AGNs are also home to many other phenomena including bright continuum and broad-line spectrum.

Radiation from the jet comes from two different processes: synchrotron radiation and inverse-Compton scattering. In synchrotron radiation, charged particles within the jet interact with the magnetic field, which changes the direction of the charged particle and causes the release of a photon. This radiation ranges all over the electromagnetic spectrum, from radio waves to gamma rays. The radiation from the synchrotron process is naturally polarized, with the direction of polarization reflecting the direction of the magnetic field in the emitting region (Rybicki & Lightman, 1979). Inverse Compton scattering occurs when fast moving charged particles from the jet collide with low energy photons. These low energy photons can have several different origins, including the cosmic microwave background (CMB), emission

line spectrum, and starlight. It is also possible that the low energy photons come from the accretion disk formed around the black hole. However, it can be argued that in the reference frame of the jet, the accretion disk would appear to be moving away at speeds close to  $c$ , and thus photon the radiation from the disk would be Doppler boosted away from the jet in the co-moving frame of the jet. Radiation from inverse-Compton scattering can also be polarized if the seed photons are polarized. In either case, high polarization suggests an ordered magnetic field (Griffiths, 1999).

Past Hubble Space Telescope (HST) and Very Large Array (VLA) observations show that the jet has very complicated morphology in radio and optical bands, revealing several distinct knots throughout the jet. Past observations show that in the inner knot region, HST-1 is varying in flux (Tsvetanov et al. 1998), in which there was an increase in flux by about 50-fold between the years of 2003-2005.

This study focuses not only on the variations in flux that have been observed in the past, but also variations in polarization. In section 2, we will discuss the instruments, observations and methods of data reduction. Section 3 will focus on results of flux measurements of several knots and how they compare with past flux measurements by Perlman et al. (2001). The section will also include the results of the optical polarization variability study. In section 4, we will discuss the physical implications on the results presented.

### 2. OBSERVATIONAL SETUP AND DATA REDUCTION

#### 2.1. HST Observations

We obtained optical polarimetry of M87's jet at 11 epochs, ranging from 1995 to 2007, with the Hubble Space Telescope (HST). Two instruments were used for these observations, the Advanced Camera for Surveys (ACS) and the Wide Field Planetary Camera (WFPC-2).

The WFPC-2 instrument, used in two observations, consists of 4 chips (PC1, WF2, WF3, WF4), arranged in a chevron. For the data sets that we present, the WF2, WF3 and WF4 chips were used as to avoid vignetting

Electronic address: mbourque@my.fit.edu, eperlman@fit.edu, mcara@fit.edu

<sup>1</sup> Southeastern Association for Research in Astronomy (SARA) NSF-REU Summer Intern

for the polarization observations, and in order to obtain images to compute the Stokes parameters. These three chips have a plate scale of  $0''.09965$  per pixel. Two filters were employed: the POLQ quad filter, which has four polarizers at 0, 45, 90 and 135 degrees (one for each chip), and either the F555W or F606W wide-band filter. Biretta (1996) describes the observational characteristics of the WFPC-2 instrument.

The ACS High Resolution Channel (HRC) detector was used for most observations, and has a considerably smaller field of view, though it does yield better resolution (plate scale  $0.028 \times 0.025''/\text{pixel}$ ). Those observations used the POL0V, POL60V and POL120V filters for polarization, along with the F606W wide-band filter. For the 2002 Dec 10 observation, the outer jet was vignettted and data was only collected on the inner and middle parts of the jet (up to knot I); for the other observations, however, the entire jet was observed. The dates and properties of each observation are summarized in Table 1.

### 2.2. Data Reduction Techniques

Raw data was retrieved from the HST data archive and recalibrated with updated flat field files and image distortion correction tables for both WFPC-2 and ACS data. The updated calibration reference files were downloaded from the STScI Calibration Database System. The data was recalibrated using standard HST calibration methods (Pavlovsky et al. 2004, Mobasher et al. 2002).

All observations were CR-split, meaning that each integration was split into two or more identical exposures in order to reject cosmic rays. MultiDrizzle, a python based script designed to reduce dithered HST images, was used to combine individual images into a single, cosmic ray rejected image for each polarizer (Fruchter & Sosey, 2009).

Drizzled images were shifted so that the core in each image was centered in the DS9 image view. Drizzled images were also rotated so that the jet was oriented with north along the y-axis. With each image centered, small shifts due to pointing jitter were found. This was done by identifying the coordinates of the core, HST-1 and several resolved globular clusters in each drizzled image and comparing them with the coordinates found of the same objects in different polarizers using IMEXAMINE. These coordinates were used in IRAF's GEOMAP and GEOTRAN functions to shift each image and correct for geometric distortions. In order to obtain the same resolution in each drizzled image, the IRAF task GAUSS was used to blur appropriate images.

Next we combined the drizzled polarizer images into Stokes I, Q, and U images. For WFPC-2 data, Stokes images were computed by using the WFPC2 Polarization Calibrator tool (Biretta, J. A.). This tool uses Mueller matrices, taking into account the polarizer used, the pick-off mirror, and the orientation of HST at the time of observation (PAV3 angle), to produce the coefficients needed to compute the Stokes images. The calibrator tool is accurate to about 1-2% (Biretta & McMaster 1997). To compute Stokes images for ACS data, a set of equations were used from the ACS data handbook (Boffi et al. 2007) that depended on the count rate, the detector, filter, and polarizer. Once Stokes U and Q images were obtained, they were used to compute the fractional

polarization

$$P = (Q^2 + U^2)^{1/2}/I \quad (1)$$

and magnetic field position angle

$$MFPA = \frac{1}{2} \times \arctan(U/Q) + 90^\circ. \quad (2)$$

In order to perform aperture polarimetry, the galaxy that made up the background in the images had to be subtracted so that no excess light be measured within an aperture. To do this, the functions ELLIPSE, BMODEL and IMCALC were used in STSDAS. ELLIPSE fits concentric isophotes using a statistical iteration method, so it was necessary to mask as many resolved globular clusters, bad pixels and defective regions as possible - as well as the jet itself. A galaxy model was then created from the ELLIPSE task and made into an image using the BMODEL function. This model was then subtracted from the Stokes I image using IMCALC.

### 2.3. Flux Apertures

Seventeen apertures used by Perlman et al. (2001) were used to test the data reduction techniques and the success of the polarization combination and galaxy fitting by measuring the fluxes of the same regions along the jet. These apertures are shown in Figure 1. Early results indicated that several of our reduction techniques had to be refined. Fluxes were not only computed to test the data reduction techniques, but were also computed to see if variations in flux through the 12 year period coincided with variations in polarization.

Aperture correction was performed for measurements in all apertures. Typically, aperture corrections are 10-20% adjustments in flux that account for the wide wings of the HST point spread function (PSF). As a result, these corrections are dependent on the structure of the source. The core and HST-1 could be modeled by PSF because of their point-like nature. To model this, the TINYTIM program was used, which generates HST PSF based on the response of the WFPC-2 and HRC detectors. Other components cannot be modeled as point sources; however, the observed flux distribution could be used. Corrections are based on the encircled energy of the detector, which is essentially the photon count in all rings of the PSF. For more detail, one can refer to chapter 5.6.3 in the ACS Instrument Handbook (Boffi et al. 2007) or Bohlin et al. 2007. Also performed for all apertures was CTE (Charge Transfer Efficiency) correction, which corrects for the efficiency or inefficiency of the transfer of charge within the detector. A perfectly efficient detector transfers 100% of the charge as the CCD registers the image. In practice, however, electrons get trapped by the silicon lattice and do not get released with the original electrons. To correct for this, we use instrumental data found in chapter 4.3.7 of the ACS Instrument Handbook (Boffi et al. 2007).

### 2.4. Aperture Polarimetry

The apertures described in Perlman et al. 2001 were also used to compute fractional polarization at first. However, first results suggested that several knots had insignificant polarization, which contrasted to the results of Perlman et al. 1999, which showed polarizations typically 20-30% in all knots, with parts of certain knots,

TABLE 1  
HST OBSERVATIONS

Date of Observation (UT)	Instrument/Detector	Filter	Polarizer	Integration Time (s)
1995 May 27	WFPC2	F555W	POLQ	5400
2002 Dec 10	ACS HRC	F606W	POL0V, POL60V, POL120V	900
2004 Dec 26	ACS HRC	F606W	POL0V, POL60V, POL120V	330
2005 Feb 9	ACS HRC	F606W	POL0V, POL60V, POL120V	330
2005 Mar 27	ACS HRC	F606W	POL0V, POL60V, POL120V	330
2005 Jun 22	ACS HRC	F606W	POL0V, POL60V, POL120V	330
2005 Aug 1	ACS HRC	F606W	POL0V, POL60V, POL120V	330
2005 Dec 26	ACS HRC	F606W	POL0V, POL60V, POL120V	330
2006 Mar 30	ACS HRC	F606W	POL0V, POL60V, POL120V	330
2006 Dec 30	ACS HRC	F606W	POL0V, POL60V, POL120V	330
2007 Nov 25	WFPC2	F606W	POLQ	480

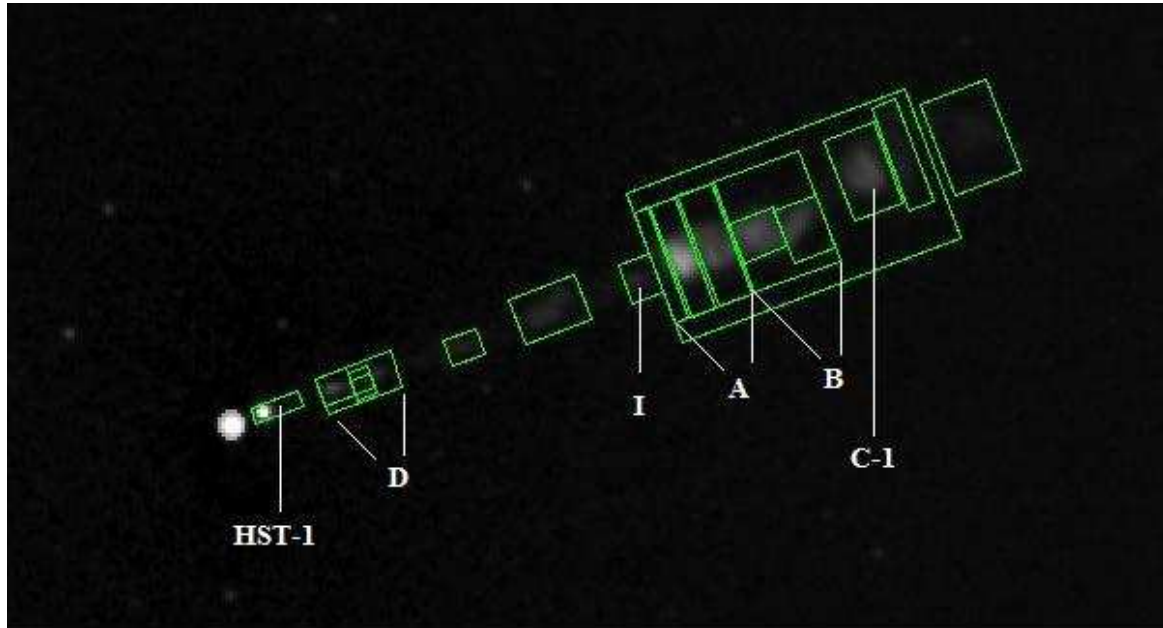


FIG. 1.— Apertures used by Perlman et al. 2001

reaching much higher values (up to  $\sim 60\%$ , Perlman et al. 1999).

The reason for the low polarization measurements was due to the fact that the apertures used by Perlman et al. 2001 were large enough to include a mixture of magnetic field position angles, and thus, a significant amount of radiation that was polarized differently. In other words, the corresponding magnetic field position angle vectors, when summed inside the aperture, led to a low measurement of polarization. For instance, our original fractional polarization measurements of knot A were on the order of 10-20%, whereas Perlman et al. 1999 measured the fractional polarization of its maximum region to be about 50%.

To avoid this issue, we created our own apertures that fit to the similar magnetic field polarization vectors shown in the contour maps of Perlman et al. 1999. Essentially, we created regions where the magnetic field position angle varied only by about 10%. In reality, these apertures were created by configuring DS9 regions. This led to the creation of 54 apertures, some including entire knot regions such as HST-1, others including only portions of knots. Though these apertures were basically

created by hand, this method does not introduce large error because we are coherently averaging the polarization values of magnetic field and position angle, similar to that of complex numbers.

CTE correction was performed for these apertures and aperture corrections were made for the core and HST-1 only. Aperture corrections were not performed for other regions of the jet because of their diffuse nature and the inability to model them with a PSF.

### 3. RESULTS

#### 3.1. Flux Variability

Flux measurements were compared to those presented in Perlman et al. 2001, which were measured from an observation performed in February of 1998. When comparing fluxes for several knots that are thought to be non-variable such as knot A, it was found that flux measurements were similar from year to year. Table 2 provides the flux measurements of HST-1, which had the greatest increase in flux of all the knots, as well as measurements for the core.

Figure 4 gives light curves for several knots along the jet. When comparing to the light curve of HST-1 pre-

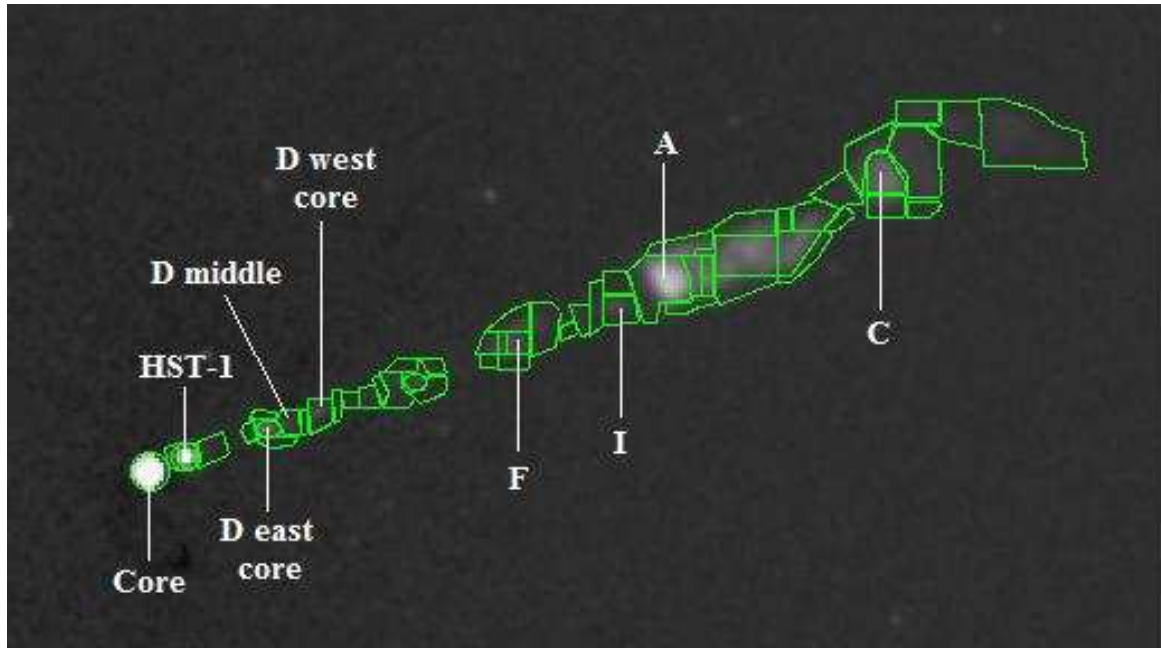


FIG. 2.— Apertures used for polarization and PA measurements

TABLE 2  
FLUX AND POLARIZATION MEASUREMENTS FOR CORE AND HST-1

Date	Core Flux	Core FP	Core MFPA	HST-1 Flux	HST-1 FP	HST-1 MFPA
1995 May 27	$781 \pm 23$	$8 \pm 3$	$-9 \pm 0$	$25 \pm 1$	$20 \pm 4$	$-69 \pm 4$
2002 Dec 10	$534 \pm 16$	$3 \pm 0$	$-90 \pm 4$	$235 \pm 7$	$39 \pm 4$	$-65 \pm 3$
2004 Dec 26	$1173 \pm 35$	$2 \pm 0$	$-51 \pm 4$	$1041 \pm 31$	$29 \pm 3$	$-57 \pm 3$
2005 Feb 9	$679 \pm 20$	$4 \pm 1$	$64 \pm 4$	$1124 \pm 34$	$36 \pm 4$	$-59 \pm 3$
2005 Mar 27	$964 \pm 29$	$6 \pm 1$	$-53 \pm 3$	$1305 \pm 39$	$43 \pm 4$	$-62 \pm 3$
2005 Jun 22	$811 \pm 24$	$10 \pm 1$	$-38 \pm 3$	$1074 \pm 32$	$33 \pm 3$	$-64 \pm 3$
2005 Aug 1	$628 \pm 19$	$7 \pm 1$	$-53 \pm 3$	$1062 \pm 32$	$36 \pm 4$	$-60 \pm 3$
2005 Dec 26	$601 \pm 18$	$4 \pm 1$	$-84 \pm 4$	$913 \pm 27$	$28 \pm 3$	$-63 \pm 3$
2006 Mar 30	$725 \pm 22$	$1 \pm 0$	$-39 \pm 12$	$615 \pm 18$	$24 \pm 3$	$-59 \pm 3$
2006 Dec 30	$905 \pm 27$	$12 \pm 1$	$-49 \pm 3$	$683 \pm 21$	$21 \pm 2$	$-60 \pm 3$
2008 Nov 25	$1616 \pm 49$	$5 \pm 3$	$41 \pm 1$	$403 \pm 12$	$20 \pm 3$	$-72 \pm 1$

sented in Harris et al. 2009, it is seen that the two results are consistent. We see a peak of the measured flux of HST-1 between the years 2004 and 2006, a secondary peak around 2007, and an overall increase in flux of about 550% between 2000 and 2005. When comparing flux results with Harris et al. 2009, it is important to note that time scales and sampling rates are significantly different.

Outside of HST-1, the other knots show little to no variability in flux. Though some graphs suggest variability, the light curves are dominated by their error bars when compared to that of HST-1. Errors in the results arise from Poisson error, error in zeropoint, and error in galaxy subtraction.

### 3.2. Optical Polarization Variability

Figure 4 gives the measured fractional polarization of several selected knots. Some regions, such as HST-1 and knot A, have high polarization (upwards of 45% and 30%, respectively) suggesting that a highly ordered magnetic field may be present. On the other hand, other regions such as the core and D east have a much lower polarization. These results are consistent with the VLA 15 GHz and HST/WFPC-2 F555W data presented by Perlman

et al. 1999 (Look at Capetti et al. 2007 for the Core polarimetry from the 2002 data). In addition to variations in flux, HST-1 is seen to be varying significantly in polarization. Between the years 2004-2006, when HST-1 was seen to have peaked in flux, the knot exhibited a peak in polarization as well. The core also shows significant, albeit less violent polarization variability at the same time that the polarization of HST-1 peaks. Though some of the other knots, particularly in the outer region of the jet, have significant polarization, there is little variability.

Figure 5 shows magnetic field position angle variability for the core and HST-1. Interestingly, despite its variability in fractional polarization, the PA for HST-1 exhibits little change and remains around 25 degrees. This is what one would expect, however, as in a simple shock, the magnetic field is commonly perpendicular to the jet (which is at an angle of -69.5 degrees). On the other hand, the PA of the core seems to change radically.

Figure 6 shows the fractional polarization versus the measured flux for the HST-1 knot. Interestingly, there seems to be a strong linear correlation between these two parameters during the observations that took place within a few years of the flux peak (2004-2006). On the

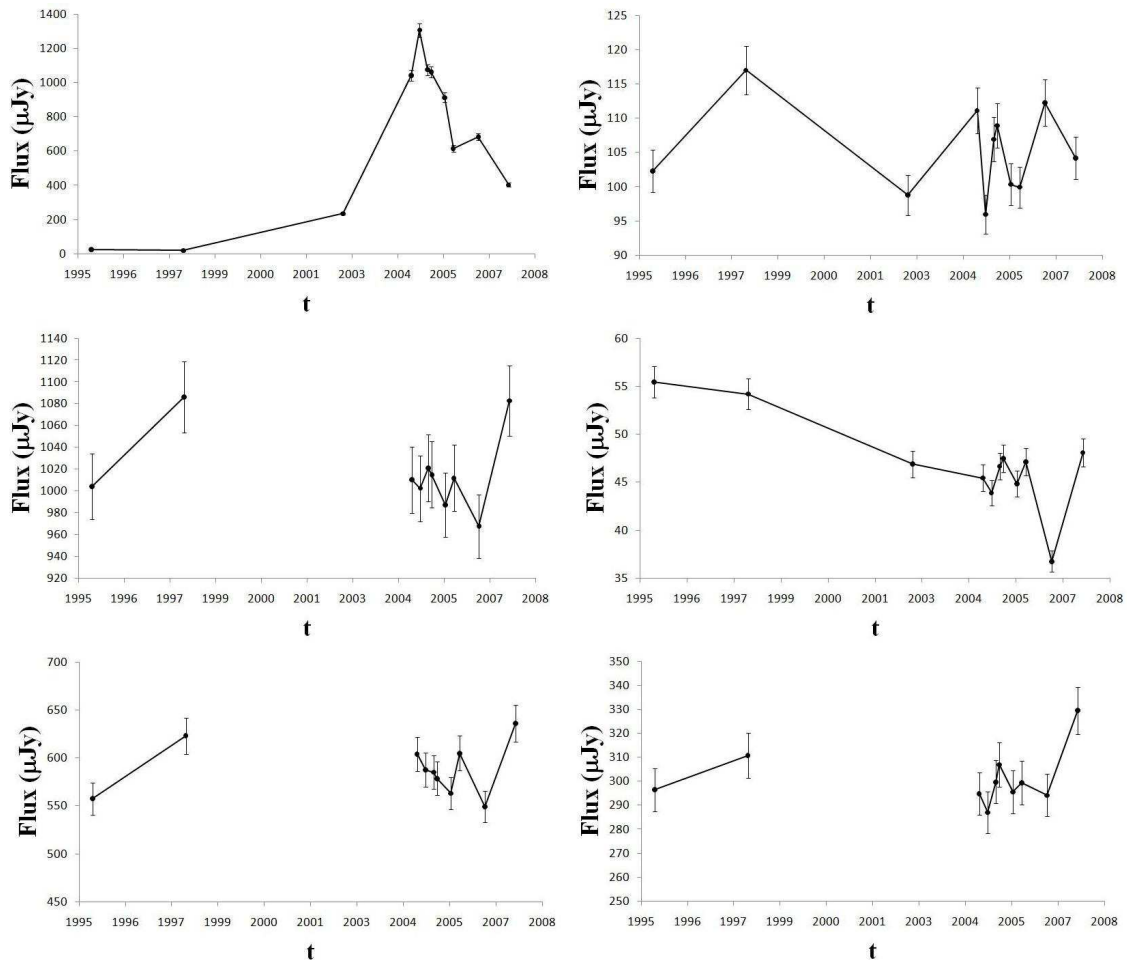


FIG. 3.— Flux variability for HST-1 (top left), knot D (top right), knot I (middle left), knot A (middle right), knot B (bottom left) and knot C-1 (bottom right)

same note, the outliers of the plot occur during 1995, 2002 and 2007, when the flux of HST-1 was not varying significantly. It is also interesting to note that, according to Madrid (2009), for essentially a three month period in 2005, the measured fluxes were basically constant (though Madrid (2009) measurements were made in the F220W and F250W band).

#### 4. DISCUSSION

The study of polarization variability in relativistic jets is a relatively new topic and has never been done in optical wavelengths with any object. Though polarization variability has been studied in some blazars (Andruchow et al., 2005, Bach et al., 2006, D’Arcangelo et al., 2009, Homan et al., 2002, Impey et al., 2000), this project is unique in that it is possible to isolate the inner knot region of the jet due to the nearness of the object.

The data that we present not only shows significant flux variations around 2005, but also significant variations in polarization around the same epoch for HST-1. On the same note, plotting polarization versus flux for this knot shows a linear correlation, especially for the epoch just described. For knots that did not vary significantly in flux, it is seen that no significant variations in polarizations were measured. However, whether or not these observations indicate strong connections between

polarization and flux is still to be determined by theorists and more observations.

Variations in polarization and magnetic field PA can indicate changes in magnetic field configurations; light will be polarized in a different way based on the orientation of the magnetic field and changes in the PA directly correspond to changes in the magnetic field. The reason for a changing magnetic field in this particular case is still highly unknown, but perhaps it could be due to changing jet dynamics or the addition of particles.

Wave disturbances along the jet could be the major contributor to the measured variations. Another reason could be the interaction between the jet and surrounding material in the ISM. Contraction or expansion of the jet could be another reason for variant polarization. In any case, it is important to note that the jet does not necessarily have to vary in strength as well; these contributions will only affect the configuration of the magnetic field. It is also important to note that special relativity predicts certain effects when viewed down a jet, including superluminal motion as well as fast and violent variability. Thus, variability can be amplified due to relativistic beaming.

Our results can have impact on verifying a model of M87 and similar galaxies in what is known as a unified scheme. Essentially, this unified scheme can describe the

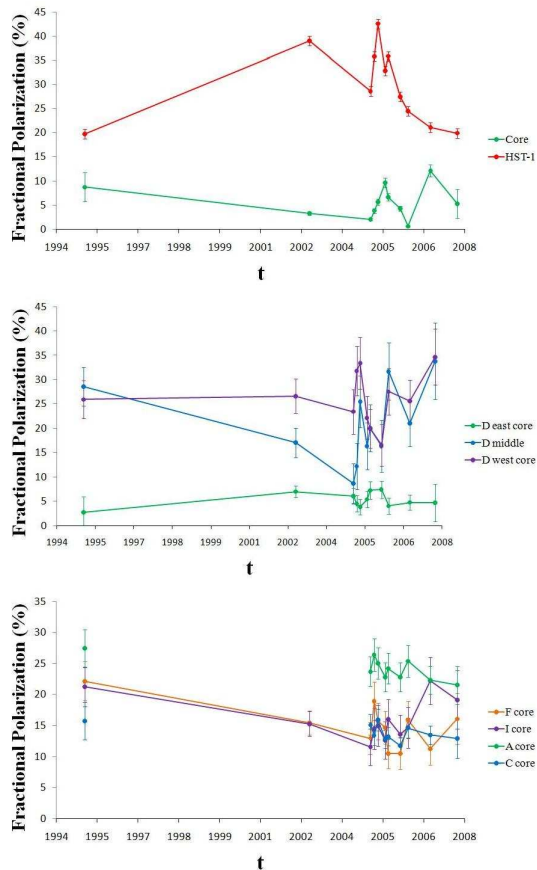


FIG. 4.— Polarization variability

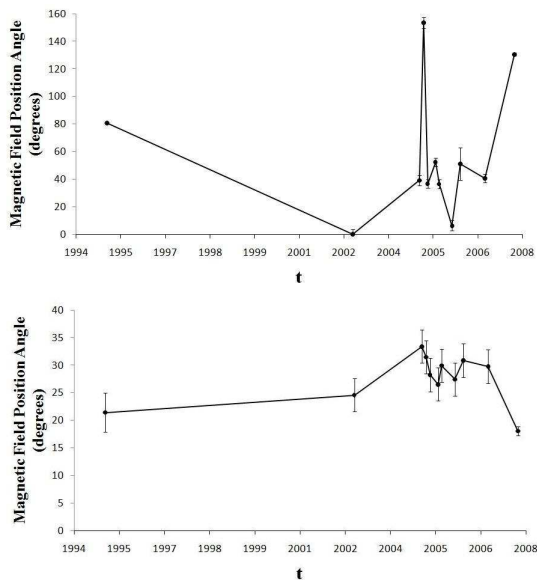


FIG. 5.— PA Variability for the Core (top panel) and HST-1 (bottom panel)

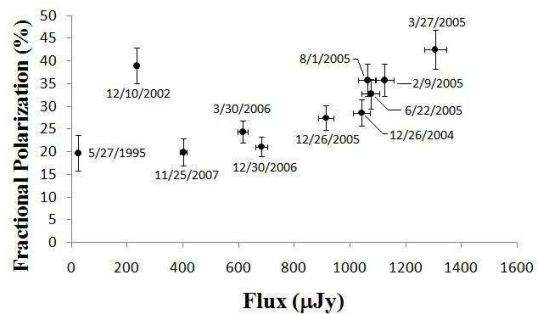


FIG. 6.— Flux vs. polarization for HST-1

nature of the radiation from the source based on the angle from which the source is observed. In active galaxies, there are several conditions in which radiation from the source could be scattered, polarized or absorbed. This is because, apart from the supermassive black hole, the accretion disk, and the jets, there are obscurations, broad-line emission clouds and narrow-line emission clouds that can affect the radiation coming from the source. Collaborators are working to improve this unified scheme in order to create a consistent model of active galaxies and to better understand what the radiation is going through (Urry, M. & Padovani, P., 1995).

## 5. CONCLUSION

The data and analysis we present show significant variations in flux as well as polarization for several distinct knots of the M87 jet, perhaps none more interesting than HST-1. Fortunately, most of our observations occurred during the two year period in which the HST-1 was undergoing its biggest changes. This study is unique in that variations in polarization have never before been measured on a quasar with such high angular resolution, unlike previous works on blazars which, due to their size and distance, do not have the angular resolution needed to isolate several distinct knots of the relativistic jet.

Future work remains on this project, not only for us but for physical theorists as well. 8 more observations of the same instruments and filters, ranging over a similar time period, are to be included in a future paper. These data sets were not included in this paper due to time constraints and the incapability of the reduction scripts to reduce dithered HST data. In addition, there is data taken in the UV band that is available and could also contribute to this project. The reduction and analysis of these extra observations will fill in some of the gaps and give us a more detailed look at the nature of the flux and polarization variations, with most of our sampling occurring near the major flare in 2005. In addition to reducing more data, we can optimize the apertures used in measuring polarization as well as the galaxy model that we subtract the background with. Changing these two parameters could yield lower errors and better results.

There is also much theoretical work that can be done with the jet of M87. The correlations that we have found between flux and polarization could perhaps lead to a self-consistent model of the jet. Long term observations could lead to information about periodicity in flares and give insight into other physical conditions of the jet.

## 6. ACKNOWLEDGMENTS

This project was funded by a partnership between the National Science Foundation (NSF AST-0552798), Research Experiences for Undergraduates (REU), and the Department of Defense (DoD) ASSURE (Awards to

Stimulate and Support Undergraduate Research Experiences) programs and NSF Major Research Instrumentation grant AST-0420753.

## REFERENCES

- Andruchow, I., Romero, G. E., & Cellone, S. A. 2005, *A&A*, 442, 97
- Bach, U., Krichbaum, T. P., Kraus, A., Witzel, A., & Zensus, J. A. 2006, *A&A*, 452, 83
- Bohlin, R. C. 2007, Instrument Science Report ACS 2007-06, 25 pages, 6
- Boffi, F.R., et al. 2007, Advanced Camera for Surveys Instrument Handbook for Cycle 17 version 8.0 (Baltimore, MD: STScI)
- Biretta, J. A. 1996, The WFPC2 Instrument Handbook (Baltimore, MD: STScI)
- Biretta, J. A., WFPC2 Polarization Calibration Tool (Baltimore, MD: STScI)
- Biretta, J. & McMaster, 1997, WFPC2 Polarization Calibration Handbook, WFPC2 Instrument Science Report 1997-11 (Baltimore, MD: STScI)
- Capetti, A., Axon, D. J., Chiaberge, M., Sparks, W. B., Duccio Macchetto, F., Cracraft, M., & Celotti, A. 2007, *A&A*, 471, 137
- D'arcangelo, F. D., et al. 2009, *ApJ*, 697, 985
- Fruchter, A. & Sosey, M., et al. 2009, MultiDrizzle Handbook Version 3.0, (Baltimore, MD: STScI)
- Griffiths, David J. 1999, "Introduction to Electrodynamics", 3rd ed. Pearson/Addison Wesley
- Harris, D. E., Biretta, J. A., Junor, W., Perlman, E. S., Sparks, W. B., & Wilson, A. S. 2003, *ApJ*, 586, L41
- Harris, D. E., Cheung, C. C., & Stawarz, L. 2007, *Bulletin of the American Astronomical Society*, 38, 936
- Harris, D. E., Cheung, C. C., Stawarz, L., Biretta, J. A., & Perlman, E. S. 2009, *ApJ*, 699, 305
- Homan, D. C., Ojha, R., Wardle, J. F. C., Roberts, D. H., Aller, M. F., Aller, H. D., & Hughes, P. A. 2002, *ApJ*, 568, 99
- Impey, C. D., Bychkov, V., Tapia, S., Gnedin, Y., & Pustilnik, S. 2000, *AJ*, 119, 1542
- Madrid, J. P. 2009, *AJ*, 137, 3864
- Mobasher, B., et al. 2002, HST WFPC2 Data Handbook Version 4.0 (Baltimore, MD: STScI)
- Pavlovsky, C., et al. 2004, ACS Data Handbook Version 3.0 (Baltimore, MD: STScI)
- Perlman, E. S., Biretta, J. A., Zhou, F., Sparks, W. B., & Macchetto, F. D. 1999, *AJ*, 117, 2185
- Perlman, E. S., Biretta, J. A., Sparks, W. B., Macchetto, F. D., & Leahy, J. P. 2001, *ApJ*, 551, 206
- Perlman, E. S., Harris, D. E., Biretta, J. A., Sparks, W. B., & Macchetto, F. D. 2003, *ApJ*, 599, L65
- Rybicki, George B. & Lightman, Alan P. 1979, "Radiative Processes in Astrophysics", Wiley
- Tsvetanov, Z. I., Hartig, G. F., Ford, H. C., Dopita, M. A., Kriss, G. A., Pei, Y. C., Dressel, L. L., & Harms, R. J. 1998, *ApJ*, 493, L83
- Urry, C. M., & Padovani, P. 1995, *PASP*, 107, 803